

Inhibition of mild steel corrosion by plant extract of *Cyperus eragrostis* Lam. in 1N Hydrochloric Acid medium

*¹Vijila Gnanaselvi G. and ²S. Velrani

^{1,2}Department of Chemistry,
Kamaraj College, Thoothukudi-628003 (India)
Affiliated to Manonmaniam Sundaranar University,
Abishekapatti, Tirunelveli-627012 (India)
*¹E-Mail: vijilagnanaselvi@gmail.com

Abstract

Inhibitory effect of plant extract of *Cyperus eragrostis* (CE) on mild steel corrosion in 1N HCl medium was investigated. Weight Loss Method, Potentiodynamic Polarization and AC impedance spectroscopy, Langmuir adsorption mechanism, FTIR and SEM were used in this present study. The experiment by Weight Loss Method has shown that the inhibition efficiency (CE) of the inhibitor increases with increase in concentration. Maximum inhibition efficiency is 87.76%. Electrochemical Impedance Spectroscopy results revealed that, the inhibition efficiency increases with increase in concentration of inhibitor and also showed that the increase of transfer resistance with inhibitor concentration. Maximum inhibition efficiency is 94.93%. In Potentiodynamic polarization measurements, Tafel polarization curve reveal that the inhibitor act as a mixed-type inhibitor and also the inhibition efficiency increases with increase in concentration. The maximum inhibition efficiency is 89.03%. Scanning Electron Microscopic analysis has provided the confirmatory evidence of the safeguard of mild steel by the green inhibitor. FTIR spectral analysis revealed that the shift in the absorption frequencies and it supports the interaction between the inhibitor and the metal surface.

Key words : *Cyperus eragrostis*, Impedance, Polarization, SEM, FTIR.

Organic inhibitors were applied extensively to protect metals from corrosion in many aggressive acidic media¹³. Naturally, plants possess, adequate cyclic organic phytochemicals nitrogen Sulphur and oxygen atoms that are responsible for their inhibition

¹20112102032005, Research Scholar, ²Assistant Professor,

properties¹⁵. Recent studies on inhibitory effect of extracts plants provided an insight on the corrosion mechanism. Potential of olive oil extract as an eco-friendly alternative to traditional corrosion inhibitors was analysed⁷. The chemical compositions and corrosion inhibition properties of the leaf extract of *Ipomoea batatas* L. (IBLE) were explored through multiple experiments, and the adsorption thermodynamic and kinetic parameters were analysed⁵. Anti-corrosive study of Raphia palm extract on mild steel in phosphoric acid solution was conducted⁴ at room temperature, under static conditions using Weight Loss, Electrochemical, and Scanning Electron Microscopy (SEM) techniques. Application of Methanol leaf extract of *Solanum macrocarpon* as a green inhibitor was analysed³. Application of *Falcaria vulgaris* (FV) leaves extract to mitigate mild steel (MS) corrosion in a 1 M HCl environment was studied⁸. Corrosion inhibitory potential of Chromolaena Odorata leaf extract (COL) on mild steel in a hydrogen Chloride acid (HCl) medium was evaluated⁶ by gravimetric method. Plants in the Cyperaceae are well known for their flavonoids, phenol, terpenoids, tannins and carbohydrates constituents. This present research work has been carried out on the problem of mild steel protection in regularly met environment i.e., HCl. This study evaluated the inhibition effect of the ethanol extract of *Cyperus eragrostis* Lam. plant on the corrosion of mild steel in 1N HCl. Present study has recorded great potential of the *C.eragrostis* plant extract for corrosion inhibition of mild steel in HCl acidic environment.

Collection of plant material :

Fresh plants of *Cyperus eragrostis*

(CE) were collected from Courtallam, Tenkasi District of Tamil Nadu, India. The plant materials were washed and dried under shadow for one week. The Earth Co-ordinates are 8.57°N 78.12°E.



Figure 1. *Cyperus eragrostis* plant

Preparation of plant extract :

The collected plants were washed carefully with distilled water to eliminate any form of dirt from the plants. The dried plants were ground with an industrial scale grinder. 20 gram of fine powder was mixed with 100 ml of ethanol and heated for 15 minutes. Then the solution was allowed to cool and settle for 24 hours. After that the cooled solution was filtered. The inhibitor test solution was prepared by using respective stock solution with different concentrations ranging from 100 to 500 ppm.

Preparation of specimens :

The specimen was prepared from cylindrical coupon cut from a mild steel rod, with the composition C:0.13%; Mn: 0.39%;

S:04%; P:0.40% and Fe, reminder and size of 3 cm×0.5cm and polished mechanically with different grades of emery papers to obtain very smooth surface. Afterwards, each and every sample was decreased using acetone wash and dried at ambient temperature. Further, they were kept at moisture-free desiccators. For the complete study, analar grade HCl and double distilled water have been used.

Weight loss method :

Corrosion rate was calculated as

$$CR = \frac{W_b - W_a}{St} \quad (1)$$

Where w_b and w_a are the specimen

weight before and after immersion in the test solution respectively, S is the surface area of the specimen, and t is the end time of each experiment. The inhibition efficiency IE (%) values were calculated from WL data by using

$$IE\% = \frac{CR^0 - CR}{CR^0} \times 100 \quad (2)$$

Where, CR^0 - corrosion rate without inhibitor

CR – corrosion rate with inhibitor

Surface coverage values were calculated also from the weight loss data by using

$$Surface\ Coverage = \frac{CR^0 - CR}{CR^0} \quad (3)$$

All the above experiments were conducted in aerated, stagnant solutions at room temperature.

Table-1. Inhibition efficiency and corrosion rate of mild steel specimens submerged in HCl acid at different temperature with and without *Cyperus eragrostis*

Test solution	Temperature (K)	Concentration (ppm)	Corrosion rate (mpy)×10 ⁻⁷	Surface coverage(θ)	Inhibition efficiency (%)
1N HCl	308	0	8.3189	-	-
		100	4.0603	0.5119	51.19
		200	2.6997	0.6754	67.54
		300	2.2498	0.7295	72.95
		400	1.8210	0.7810	78.10
		500	1.0177	0.8776	87.76
	313	0	9.7492	-	-
		100	5.3245	0.4538	45.38
		200	3.7389	0.6264	62.64
		300	2.9623	0.6961	69.61
		400	2.2945	0.7677	76.77
		500	1.9819	0.7967	79.67
	318	0	13.7614	-	-
		100	8.0779	0.4130	41.30
		200	6.1923	0.5500	55.00
		300	4.4785	0.6749	67.49
		400	3.6800	0.7325	73.25
		500	2.9836	0.7832	78.32

	323	0	36.018	-	-
		100	23.044	0.3602	36.02
		200	16.536	0.5408	54.08
		300	13.1507	0.6348	63.48
		400	10.0277	0.7216	72.16
		500	8.672	0.7760	77.60
	328	0	74.233	-	-
		100	54.911	0.2602	26.02
		200	37.813	0.4906	49.06
		300	30.720	0.5861	58.61
		400	22.160	0.7014	70.14
		500	17.441	0.7650	76.50

Table-1 shows the corrosion rate, surface coverage and inhibition efficiency of the inhibitor *Cyperus eragrostis* plant extract. The measurements were taken at different temperatures ranging from 308K to 328K. In this specific analysis, the steel specimens were immersed for 4 hours. From the results it is found that, the immersion rate decreased with inhibitor concentration. It is also to be noted that when temperature increases the corrosion rate also increases. The immersion efficiency of the plant extract of *Cyperus eragrostis* is 87.76 % at 308K for the concentration of 500ppm.

Thermodynamic studies :
Arrhenius curve :

Thermodynamic factors of enthalpy of activation (ΔH), entropy of activation (ΔS) and apparent activation energy (E_a) were measured using the following Arrhenius equation for corrosion of mild steel in 1N HCl solutions in the absence and presence of CE at temperature range from 308 K to 328 K.

$$CR = A \exp(-E_a/RT) \quad (4)$$

It is possible to derive the logarithm of both sides of the given equation.

$$\log CR = \log A - E_a/2.303RT \quad (5)$$

The transition state equation was used to calculate the change in enthalpy [ΔH] and entropy [ΔS] for the production of the activated complex

$$\log CR/T = \{(\log R/hN + (\Delta S)/2.303 R)\} - \Delta H/2.303 RT \quad (6)$$

Here CR and A are the corrosion rate and pre-exponential factor, h and N are the Planck's constant and Avogadro's number, E_a is the apparent activation energy, gas constant is denoted as R ($R = 8.314 \text{ J mol}^{-1} \text{ K}^{-1}$) and T is the temperature in K. As shown in Figure 2, the plot of $\log CR$ vs $1/T$ of 1N HCl produced a straight line with a slope ($-E_a/2.303 R$) and intercept ($\log A$). In acid medium 1N HCl, the values of E_a obtained in solutions containing CE extracts may be regarded as physical adsorption¹⁰. The ΔH and ΔS were determined using the slope ($-\Delta H/2.303R$) and intercept ($\log R/hN + (\Delta S)/2.303 R$) of the plot of $\log CR/T$ vs. $1/T$ as shown in Figure 3. Moreover, the calculated values of ΔH and ΔS were presented in Table-2.

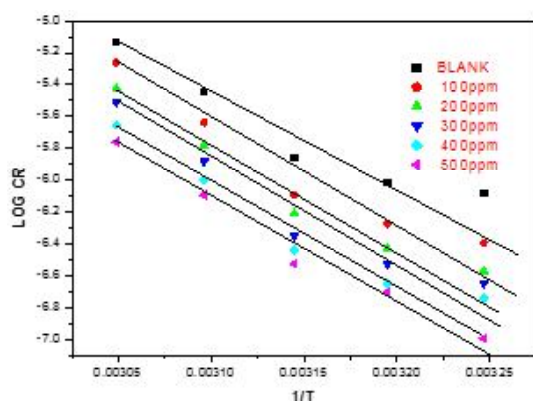


Figure 2. Arrhenius curves of log CR against 1/T in 1N HCl at different concentrations of CE

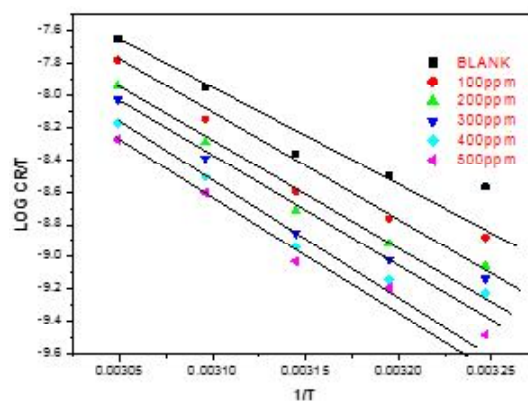


Figure 3. Transition state plots of log CR/T against 1/T at various concentrations of CE in 1N HCl

From these data, it is found that the thermodynamic parameters such as ΔH and ΔS of dissolution reaction of mild steel in 1N HCl in the presence of CE were higher than the uninhibited solution. The positive values of ΔH clearly confirmed the endothermic nature of the steel dissolution process². The ΔS values

were negative in both the absence and presence of tested inhibitor. Moreover, the activated complex in the rate-determining phase was a dissociation step rather than an association step, confirming that the decrease in disordering takes place when reactants converted to activate complex.

Table-2. Corrosion kinetic factors for mild steel in 1N HCl in the absence and presence of various concentrations of CE

Concentration(ppm)	E_a (KJ/mol)	ΔH (KJ/mol)	ΔS (J/mol/K)
0	95.02	92.11	-28.17
100	111.62	108.71	-25.66
200	113.25	110.35	-25.55
300	112.38	109.47	-25.79
400	108.65	105.75	-26.51
500	118.82	115.91	-24.96

Langmuir adsorption isotherm :

Langmuir adsorption isotherm equation is shown as

$$\text{Log} \left(\frac{\theta}{1-\theta} \right) = \text{log } C + \text{log } K_{ads} \quad (7)$$

Where, C is a concentration of inhibitor, θ is a fraction of surface coverage area, K_{ads} is adsorption equilibrium constant.

When a graph is plotted between log C and log $\theta/(1-\theta)$, a straight line ($R^2 > 0.9$) is

obtained as shown in Figure 4 with gradient slope equal to one and intercept equal to $\log K_{ads}$. The gradient is not unity Langmuir adsorption isotherm indicates that the organic components present in the plant extracts having polar atom or groups are adsorbed on the metal surface may interact by mutual repulsion or attraction⁹.

The collected data is presented in Table-3. The adsorption studies clearly revealed that the experimental data fitted the Langmuir adsorption isotherm with a correlation coefficient greater than 0.90. The negative values of ΔG in Table-3 revealed the spontaneous CE adsorption on the mild steel surfaces and poor interaction between metal surface and inhibitor molecules¹⁴. Physisorption is often defined as values of ΔG_{ads} up to -20kJ/mol, which is compatible with electrostatic interaction between the metal surface and charged molecules¹¹. If the ΔG_{ads} values are around -40KJ/mole or higher, charge transfer

or sharing takes place on the metal surface from inhibitor molecules through coordinate bond. The ΔG_{ads} values are below -20 KJ/mol in acid medium in this present study. Therefore, the physisorption played a significant role on the adsorption mechanism of CE on Mild Steel in 1N HCl solution at investigated temperature range.

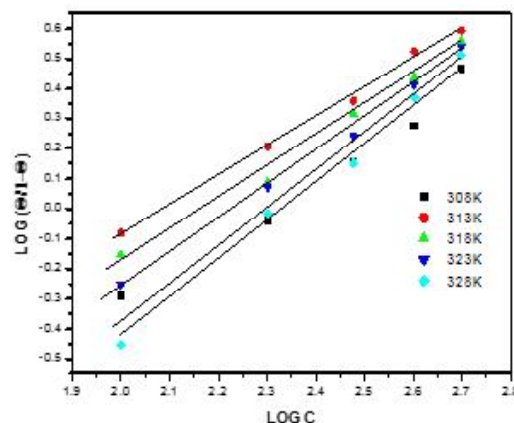


Figure 4. Langmuir adsorption isotherm plot of corrosion on mild steel in the presence of CE extract

Table-3. Thermodynamic data for CE for Langmuir adsorption isotherm

Temperature (K)	Intercept	Slope	R ²	ΔG (KJ/mol)	K_{ads}
308	-2.415	1.0468	0.9796	-3.95	3.85×10^{-3}
313	-2.0374	0.9761	0.9968	-1.75	9.17×10^{-3}
318	-2.2271	1.0251	0.9909	-2.94	5.93×10^{-3}
323	-2.4937	1.1163	0.9959	-4.63	3.21×10^{-3}
328	-3.1694	1.3587	0.9947	-8.97	6.77×10^{-4}

Electrochemical studies :

Potential-Dynamic Polarization Study :

The percentage of inhibition efficiency (IE) was calculated from I_{corr} values using the equation:

$$IE\% = \frac{[I_{corr}(Blank) - I_{corr}(inh)]}{[I_{corr}(blank)]} \times 100 \quad (8)$$

Where $I_{corr}(blank)$ and $I_{corr}(inh)$ are the corrosion current density¹ values without and with inhibitor respectively. All electrochemical measurements were carried out at 308K using 100ml of electrolyte in a stationary condition.

Table-4. Potentiodynamic polarization parameters for the corrosion of mild steel in 1N HCl without and with different concentration of Cyperus eragrostis

C_{inh} (M)	E_{corr} (mV)	i_{corr} (Acm^{-2}) $\times 10^{-4}$	b_a (mV/decade)	b_c (mV/decade)	%IE
Blank	-0.5234	8.324	8.896	7.150	-
100	-0.5008	6.697	9.430	7.992	19.54
200	-0.4935	3.232	10.130	8.991	61.17
300	-0.4799	1.496	11.223	9.531	82.02
400	-0.4778	1.366	11.838	10.158	83.59
500	-0.4678	0.9124	13.057	10.383	89.03

Potentiometric polarization curves of mild steel in absence and presence of various concentrations of the plant extract in 1N HCl are shown in Figure 5 as Tafel plot. Table-4 shows that, with the increase in concentration of inhibitors the value of current density increases. This indicates that the inhibitor reduces the corrosion rate.

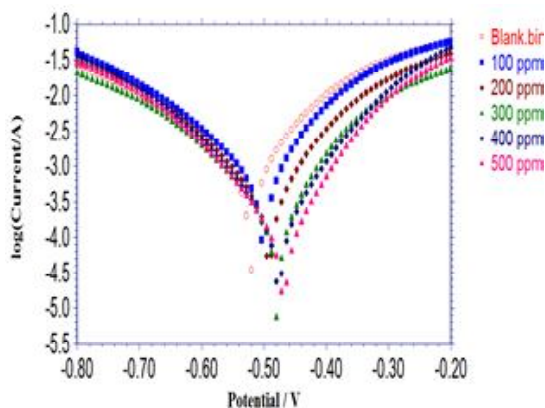


Figure 5. Tafel Plot for mild steel immersed in 1N HCl at different concentrations of CE at 308K

Electrochemical Impedance Measurements:

The inhibition efficiencies for each concentration were calculated using the

formula:

$$IE\% = \frac{R_{ct} - R_{ct}^0}{R_{ct}} \times 100 \quad (9)$$

Where R_{ct}^0 and R_{ct} are the charge transfer resistance in the absence and presence of inhibitor respectively. The double layer capacitance (C_{dl}) was calculated by using the formula

$$C_{dl} = \frac{1}{2\pi f_{max} R_{ct}} \quad (10)$$

Where f_{max} is the frequency at maximum in the Nyquist plot¹². Each experiment was run in triplicate to check the reproducibility of the data

Mechanism :

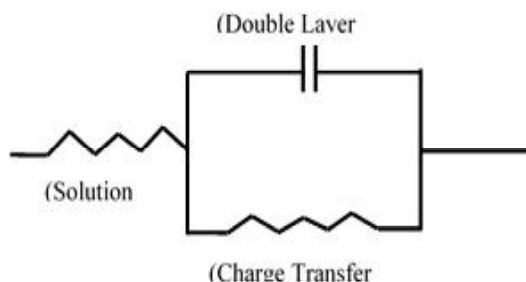


Figure 6. An equivalent circuit Mechanism for Impedance Analysis

Table-5. Electrochemical impedance parameters for mild steel in 1N HCl without and with different concentrations of Cyperus eragrostis

Inhibitor concentration (ppm)	$R_{CT}(\Omega\text{cm}^2)$	$F_{\max}(\text{HZ})$	$R_s(\Omega\text{cm}^2)$	$C_{dl}(\text{Fcm}^{-2})$	%IE
Blank	5.516	0.2759	2.939	0.001704	-
100	19.47	0.9750	2.459	0.00011	71.67
200	53.97	2.700	3.241	0.0002321	89.78
300	82.26	4.088	5.918	0.0002164	93.29
400	88.55	4.437	2.423	0.0002637	93.77

The Nyquist plot is given in Figure 7. The plot reveals that the corrosion process is under activation control. In Figure 7, there is a semicircle indicating the charge transfer process during corrosion process. The charge transfer resistance, R_{ct} values are from 5.516 to 108.8 Ωcm^{-2} in 1N HCl.

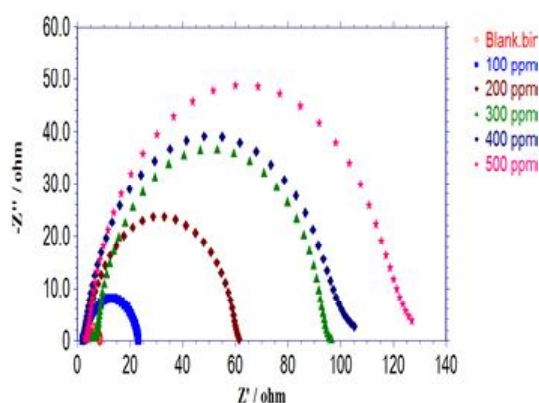


Figure 7. Nyquist Plot for mild steel immersed in 1N HCl at different concentrations of CE at 308K

Morphological studies :
FT-IR Spectral Analysis :

FTIR spectra for Cyperus eragrostis plant extract and the dried product formed

between finely powdered mild steel specimen and the concentrated solutions of the extract was recorded in Shimadzu-FTIR-8400S spectrophotometer. FT-IR spectral studies were carried out for adsorbed layer formed on the mild steel in 1N HCl in the absence of inhibitor and also adsorbed layer formed on the mild steel in 1N HCl in the presence of inhibitor. It is shown in figure 8. Their respective FT-IR peaks are given in Table-6.

Table-6. Frequencies and assignment of adsorption of FTIR spectra for adsorbed layer formed on the mild steel in 1N HCl in the absence and presence of inhibitor

Mild steel in 1N HCl in the absence of the inhibitor (cm^{-1})	Mild steel in 1N HCl in presence of inhibitor (cm^{-1})	Assignment
3129.95	3124.19	O-H Stretching
1740.30	1736.21	C=O Stretching
1634.05	1638.14	C=N Stretching
1400.14	1400.40	C-N Stretching
1033.37	1052.15	C-O Stretching

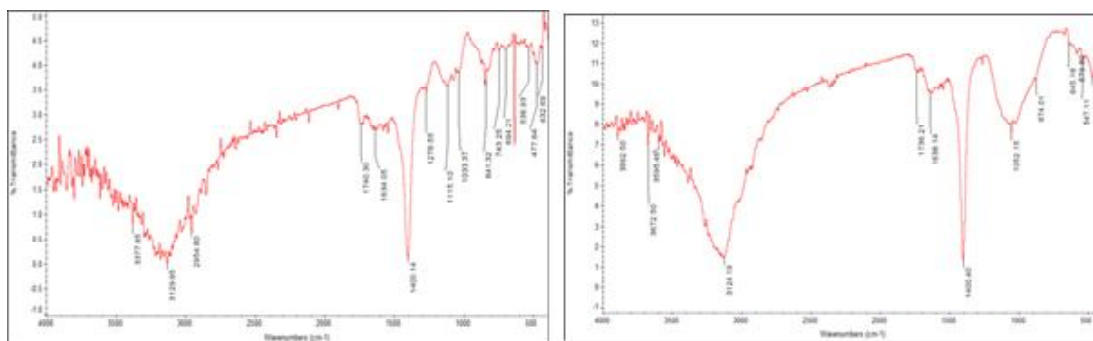


Figure 8. FT-IR spectra of adsorbed layer formed on the mild steel in 1N HCl in the absence and the presence of inhibitor

From the Table-6 it is observed that the frequencies and assignment of adsorption of FTIR spectra for adsorbed layer formed on the mild steel in 1N HCl in the absence and presence of inhibitor *Cyperus eragrostis* plant extract are shifted. O-H (shifted from 3129.95 to 3124.19 cm^{-1}), C=C (Shifted from 1740.30 to 1736.21 cm^{-1}), C=N (shifted from 1634.05 to 1638.14 cm^{-1}), C-N (shifted from 1400.14 to 1400.40 cm^{-1}), S-O (shifted from 1033.37 to 1052.15 cm^{-1}). The shift in the absorption frequencies of the inhibitor on the metal surface supports the interaction between the inhibitor and the metal surface.

Morphological studies :

SEM Analysis :

Scanning Electron Microscopy (JEOL, JSM 6390) was used to evaluate the nature of the surface layer produced on the assured samples. SEM images of mild steel surfaces after 24 hours of immersion in 1N HCl in the absence and presence of CE are shown in Figure 9. The specimens were taken out after 24 hours and dried. The surface of the inhibited mild steel specimens was better than the

uninhibited sample, according to SEM photographs. The corrosion rate was lowered in the presence of inhibitors according to these findings. The adsorption of inhibitor molecules on the metal surface as a protective layer reduces the rate of corrosion.

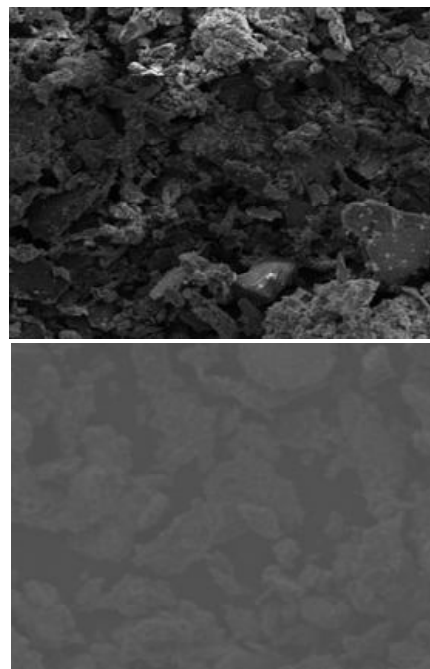


Figure 9. SEM Images of Mild steel in 1 N HCl in the absence of inhibitor and in the presence of inhibitor.

The measurements were taken by Weight loss method at different temperatures ranging from 308K to 328K with different concentrations blank to 500 ppm of HCl. The immersion efficiency of the plant extract of *Cyperus eragrostis* is 87.76 % at 308K for the concentration of 500ppm. From the Thermodynamic studies it is found that the thermodynamic parameters such as ΔH and ΔS of dissolution reaction of mild steel in 1N HCl in the presence of CE were higher than the uninhibited solution. The positive values of ΔH clearly confirmed the endothermic nature of the steel dissolution process. Langmuir adsorption isotherm studies were conducted from 308 K to 328 K in steps of 5 K. The ΔG_{ads} values are below -20 KJ/mol in acid medium in this present study. Therefore, the physisorption played a significant role on the adsorption mechanism of CE on Mild Steel in 1N HCl solution at investigated temperature range. Tafel Plot for mild steel immersed in 1N HCl at different concentrations of CE at 308K was drawn by using Potentio-Dynamic Polarization Study. The IE is 89.03% at 500ppm of inhibitor concentration. Electrochemical Impedance Measurements were carried out and Nyquist plot was drawn. The plot reveals that the corrosion process is under activation control. Maximum inhibition efficiency is 94.93%. There is a semicircle indicating the charge transfer process during corrosion process. FT-IR spectral studies were carried out for adsorbed layer formed on the mild steel in 1N HCl in the absence of inhibitor and also adsorbed layer formed on the mild steel in 1N HCl in the presence of inhibitor. The shift in the absorption frequencies of the inhibitor on the metal surface supports the interaction between the inhibitor and the metal surface. SEM images of mild steel surfaces after 24 hours of immersion in

1N HCl in the absence and presence of CE are taken. The surface of the inhibited mild steel specimens was better than the uninhibited sample, according to SEM photographs. The adsorption of inhibitor molecules on the metal surface as a protective layer reduces the rate of corrosion. Obtained findings in the present study clearly demonstrates that the CE effectively inhibits the corrosion of mild steel in 1N HCl. In acid medium, the CE acts as a mixed type of inhibitor and this statement was confirmed by the Potentiodynamic polarization results.

References :

1. Akbar Ali Samsath Begum, Raja Mohamed Abdul Vahith, Vijay Kotra, Mohammed Rafi Shaik, Abdelatty Abdelgawad, Emad Mahrous Awwad, Mujeeb Khan, (2021), *Coatings*, 11(1): 106. <https://doi.org/10.3390/coatings11010106>
2. Al-Amiery, A.A., A.B. Mohamad, and A.A.H. Kadhum (2022) *Scientific Reports*, 12: 4705. <https://doi.org/10.1038/s41598-022-08146-8>.
3. Alimohammadi, M., M. Ghaderi and S.A.A. Ramazani (2023), *Scientific Reports*, 13: 3737. <https://doi.org/10.1038/s41598-023-30571-6>
4. Amine, J D, T J Ikyuve, and A Ashwe, (2023), *Journal of Material Science and Metallurgy*, 4 (1): 1-10.
5. Bi-lan Lin, Xin-xin Zhou, Tian-hu Duan, Chen Zhao, Jia-hao Zhu, Yu-ye Xu, (2024), *Journal of Chemistry*, 17(1): 105410, <https://doi.org/10.1016/j.arabjc.2023.105410>.
6. Elhady, S., H. Inan, and M. Shaaban, *et al.* (2023), *Scientific Reports*, 13: 17151. <https://doi.org/10.1038/s41598-023-43701-x>
7. Ezech E. M., and Agu P Chinedu, (2023),

- Moroccan Journal of Chemistry*, 14(1): 188-204. Doi: <https://doi.org/10.48317/IMIST.PRSM/morjchem-v10i3.30521>
8. Ezugha, S.I., and C.C. Aralu, (2023), *SN Applied Sciences*, 2023; 5: 381. <https://doi.org/10.1007/s42452-023-05594-3>
 9. Fatma M. Mahgoub, M. Ahmed, Eman H. Hefnawy, and Abd Alrazzaq, (2019), *Desalination and Water Treatment*, 169: 49-58, doi: 10.5004/dwt.2019.24681.
 10. Ogunleye, Arinkoola, Eletta, Agbede, Osho, Morakinyo, and Hamed, (2020), *Heliyon*, 6(1): 03205. <https://doi.org/10.1016/j.heliyon.2020.e03205>.
 11. Perumal S, Kannan R Sayee, S Muthumanickam, A Elangovan, N Muniyappan, and K K Mothilal, (2022), *Journal of Advanced Scientific Research*, 13 (3): 151-160, <https://doi.org/10.55218/JASR.202213324>.
 12. Pourzarghan, V., and B. Fazeli-Nasab, (2021), *Heritage Science*, 9(75): 1-14. <https://doi.org/10.1186/s40494-021-00545-w>.
 13. Suchitra Chaudhary, and Rakesh K. Tak, (2022), *Biointerface Research in Applied Chemistry*, 12 (2): 2603-2617, <https://doi.org/10.33263/BRIAC122.26032617>
 14. Suraj B. Ade, (2022), *International Journal for Research in Applied Science & Engineering Technology*, 10 (3): 136-147. <https://doi.org/10.22214/ijraset.2022.40582>.
 15. William-Ebi Duduna, Osaribie Nelson Akeme, and Tombiri Mark Zinipere, (2019), *International Journal Of Scientific & Technology Research*, 8(8).